RESEARCH ARTICLE | *Neurogastroenterology and Motility*

Enteric neuron density correlates with clinical features of severe gut dysmotility

Elisa Boschetti,[1] Carolina Malagelada,[2] Anna Accarino,[2] Juan R. Malagelada,[2] Rosanna F. Cogliandro,[1] Alessandra Gori,[1] Elena Bonora,[1] Fiorella Giancola,[1] Francesca Bianco,[1] Vitaliano Tugnoli,[3] Paolo Clavenzani,[4] 🄳 Fernando Azpiroz,[2] Vincenzo Stanghellini,[1] Catia Sternini,[5] and Roberto De Giorgio[6]

[1]*Department of Medical and Surgical Sciences, University of Bologna, Bologna, Italy;* [2]*Digestive System Research Unit, University Hospital Vall d'Hebron, Centro de Investigación Biomédica en Red de Enfermedades Hepáticas y Digestivas (Ciberehd), Barcelona, Spain;* [3]*Department of Biomedical and Neuro Motor Sciences, University of Bologna, Bologna, Italy;* [4]*Department of Veterinary Medicine, University of Bologna, Ozzano, Italy;* [5]*Digestive Disease Division, Departments of Medicine and Neurobiology, University of California, Los Angeles, California; and* [6]*Department of Medical Sciences, University of Ferrara, Ferrara, Italy*

Boschetti E, Malagelada C, Accarino A, Malagelada JR, Cogliandro RF, Gori A, Bonora E, Giancola F, Bianco F, Tugnoli V, Clavenzani P, Azpiroz F, Stanghellini V, Sternini C, De Giorgio R. Enteric neuron density correlates with clinical features of severe gut dysmotility. *Am J Physiol Gastrointest Liver Physiol* 317: G793–G801, 2019. First published September 23, 2019; doi:10.1152/ajpgi. 00199.2019.—Gastrointestinal (GI) symptoms can originate from severe dysmotility due to enteric neuropathies. Current methods used to demonstrate enteric neuropathies are based mainly on classic qualitative histopathological/immunohistochemical evaluation. This study was designed to identify an objective morphometric method for paraffin-embedded tissue samples to quantify the interganglionic distance between neighboring myenteric ganglia immunoreactive for neuron-specific enolase, as well as the number of myenteric and submucosal neuronal cell bodies/ganglion in jejunal specimens of patients with severe GI dysmotility. Jejunal full-thickness biopsies were collected from 32 patients (22 females; 16–77 yr) with well-characterized severe dysmotility and 8 controls (4 females; 47–73 yr). A symptom questionnaire was filled before surgery. Mann-Whitney *U* test, Kruskal-Wallis coupled with Dunn's posttest and nonparametric linear regression tests were used for analyzing morphometric data and clinical correlations, respectively. Compared with controls, patients with severe dysmotility exhibited a significant increase in myenteric interganglionic distance ($P = 0.0005$) along with a decrease in the number of myenteric ($P < 0.00001$) and submucosal ($P < 0.0004$) neurons. A 50% reduction in the number of submucosal and myenteric neurons correlated with an increased interganglionic distance and severity of dysmotility. Our study proposes a relatively simple tool that can be applied for quantitative evaluation of paraffin sections from patients with severe dysmotility. The finding of an increased interganglionic distance may aid diagnosis and limit the direct quantitative analysis of neurons per ganglion in patients with an interganglionic distance within the control range.

NEW & NOTEWORTHY Enteric neuropathies are challenging conditions characterized by a severe impairment of gut physiology, including motility. An accurate, unambiguous assessment of enteric neurons provided by quantitative analysis of routine paraffin sections may help to define neuropathy-related gut dysmotility. We showed that patients with severe gut dysmotility exhibited an increased interganglionic distance associated with a decreased number of myenteric and submucosal neurons, which correlated with symptoms and clinical manifestations of deranged intestinal motility.

chronic intestinal pseudo-obstruction; enteric neuron cell count; interganglionic distance; severe gut dysmotility

INTRODUCTION

Severe gut dysmotility is a clinical condition with pronounced impairment of gut propulsion induced by alterations of enteric neurons and/or glial cells, interstitial cells of Cajal (ICC), and muscle cells in the gastrointestinal (GI) tract (8, 23). Chronic intestinal pseudo-obstruction (CIPO), characterized by severe and recurrent subocclusive episodes with clinical and radiological findings mimicking mechanical obstruction, is a particularly challenging and morbid form of severe dysmotility (7, 33). Patients with CIPO manifest severe symptoms (e.g., chronic nausea, vomiting, abdominal distension, and constipation/diarrhea) responsible for body weight loss, often requiring intravenous nutritional support (9). In addition to CIPO, severe dysmotility includes severe functional GI disorders, also referred to as enteric dysmotility; these patients present with severe motility impairment symptoms, nutritional defects, and impaired quality of life similar to CIPO but without intestinal subocclusive episodes (7, 22, 35).

A recent study by our group, comparing small bowel manometric abnormalities with histopathological findings in full-thickness intestinal biopsies (24), showed that ~38% of the patients with a neuropathic manometric pattern compatible with severe dysmotility had apparently normal histopathology. However, our results did not establish a correlation between intestinal manometry and histopathology. This unexpected finding might be explained by the qualitative approaches traditionally used to demonstrate pathological changes throughout the enteric neuromuscular layer in full-thickness biopsies, which are not standardized and depend on an individual pathologist's expertise, often limited, with few exceptions. Indeed, histopathology reporting and interpretation criteria are

extremely subjective (3, 11). In clinically challenging conditions, quantitative histopathological analysis may provide a better definition of the underlying neuromuscular disease by revealing abnormalities that, although subtle, may bear diagnostic implications.

The best strategy for a reliable quantitative analysis of enteric neurons is to use whole mount preparations containing the myenteric and submucosal plexuses with neuronal cell bodies identified by panneuronal immunohistochemical markers (4, 14, 17, 20, 26). However, this approach, which is often used in experimental animal models and in the research setting, is not conveniently applicable in human routine pathology. Indeed, virtually all surgical specimens are processed using formalin fixation followed by paraffin inclusion (27). This routine method is reliable for pathological assessment, is convenient for long-term storage of the processed material, and entails limited costs. Furthermore, formalin-fixed, paraffin-embedded material can be sectioned by microtome and sections can be often exchanged from one laboratory to another for referral, second evaluation and retrospective examination (10, 17). Thus, we considered such formalin-fixed, paraffin-embedded specimens potentially suitable for neuron quantification.

The enteric nervous system exerts a dominant regulatory role in the gut, making reliable quantitative enteric neuronal analysis a major target in any pathological evaluation of gut specimens of patients with neuromuscular disorders. Nonetheless, methodological criteria aimed at quantifying and assessing the density of enteric neurons are still largely debated, since an accurate evaluation of neuronal cell populations in paraffin-embedded intestinal samples remains challenging. This study was designed to establish a quantitative method using a panneuronal marker to analyze the number of neurons per ganglion in submucosal and myenteric plexuses along with the distance between myenteric adjacent ganglia in jejunal full thickness, formalin-fixed, paraffin-embedded biopsies from patients with well-characterized severe gut dysmotility. We also tested for possible correlations between morphometric results and symptoms and clinical signs detectable in the enrolled patients.

MATERIALS AND METHODS

Patients. Thirty-two patients with severe dysmotility (22 females; age range 16–77 yr) were clinically evaluated at the Vall d'Hebron University Hospital in Barcelona and recruited for this study between November 1999 and November 2009. Patients underwent abdominal surgery or laparoscopy, and full-thickness biopsies of the jejunum were obtained. Patients with motility disorders secondary to infectious, neurological, metabolic, autoimmune, and paraneoplastic conditions were excluded. Anorexia nervosa was ruled out in all patients with malnutrition via psychiatric referral. The clinical diagnosis of CIPO (*n* = 19; 12 females; age range 16–77 yr) and enteric dysmotility (*n* = 13; 10 females; age range 25–52 yr) was established as previously described (24). Control patients (*n* = 8; 4 females; age range 47–73 yr) underwent abdominal surgery for noncomplicated neoplastic tumor. Full-thickness biopsies were collected in the adjacent jejunal tissue showing neither macroscopic nor microscopic abnormalities. Each patient and control subject answered a symptom questionnaire before surgery. The following data were collected: age, sex, body mass index (BMI), need for parenteral nutrition, central venous catheter-related infections, number of subocclusive episodes (before surgery for each patient), abdominal distension, abdominal

pain, nausea, vomiting, fullness, sensation of early satiety, and constipation and/or diarrhea according to the Bristol stool scale. Extraintestinal motor abnormalities, such as esophageal involvement and occurrence of gastroparesis, were also assessed. Finally, the presence of small intestinal bacterial overgrowth (SIBO), urinary symptoms and age of symptom onset were evaluated by anamnesis and pertinent diagnostic tests.

The study protocol was approved by the Ethics Committee of the University Hospital Vall d'Hebron, Barcelona, Spain, and the Ethics Committee of St. Orsola-Malpighi Hospital of Bologna, Italy (EM/146/2014/O). All patients gave written informed consent.

Intestinal tissue sampling. Full-thickness biopsy specimens were obtained from the proximal jejunum either by laparoscopy or by conventional laparotomy. In each patient, a single circular segment (5 cm long) was collected. Immediately after resection, specimens were fixed in 10% formalin overnight, embedded in paraffin, and sectioned (5 μm) according to the standard protocol for tissue processing.

Histopathology. A qualitative histopathological review was conducted as previously described (24). Paraffin-embedded jejunal cross sections were rehydrated, antigen retrieval was performed heating sections 25 min at 90°C in a water bath in the presence of 10 mmol/L sodium citrate buffer pH 6.0 (Carlo Erba, Milan, Italy). Sections were treated with an endogenous peroxidase blocking kit (Gene Tex, Aachen, Germany). Immunostaining was performed using a commercial kit (Millipore, Milan, Italy) following the manufacturer's instructions.

Histopathological material was examined blindly without prior information about clinical and motility test outcomes. All biopsies were first analyzed to exclude associated pathological findings such as malignancy, dysplasia, or villous atrophy. Routine histochemical staining was used to evaluate the enteric neuromuscular architecture. Immunohistochemical labeling was used to identify specific enteric neuromuscular component according to standardized and well-validated protocols (17). The following antibodies were used: *1*) panneuronal marker: neuron-specific enolase (NSE; rabbit PA1-28217, ready to use antibody; Thermo Fisher Scientific, Rockford, IL) and synaptophysin (rabbit A0010, dilution 1:100; DAKO, Glostrup, Denmark); *2*) marker of cell survival: BCL-2 (mouse M0887, dilution 1:100, DAKO); *3*) marker of glial cells: S100β (rabbit Z0311, dilution 1:400, DAKO); *4*) marker of ICC: c-Kit (rabbit A4502, dilution 1:400, DAKO); *5*) marker of smooth muscle cells: α-smooth muscle actin (α-SMA; mouse M0851, dilution 1:400, DAKO); *6*) markers of T lymphocyte subsets: CD45 (leukocytes; mouse M0834, dilution 1:40, DAKO), CD3 (general T lymphocyte marker; rabbit A0452, dilution 1:25, DAKO), and CD8 (mouse M7103, dilution 1:50, DAKO; and *7*) marker of mast cells: anti-tryptase antibody (mouse M7052, dilution 1:800, DAKO).

The immunohistochemical evaluation of neurons, glial cells, muscle cells, ICC, and immune cells allowed us to stratify the patients. Three histopathological patterns were recognized in patients' specimens according to the London classification (19):

1) apparently normal (AN): (*n* = 10; 7 females; age range: 24–61 yr) no detectable changes in the neuromuscular layer;

2) inflammatory neuromyopathy (INF): (*n* = 14; 10 females; age range: 16–77 yr) characterized by neuromuscular-glial-ICC alterations with an inflammatory infiltrate throughout the neuromuscular layer; and

3) degenerative neuromyopathy (DEG): (*n* = 8; 5 female; age range: 29–70 yr) characterized by neuromuscular-glial-ICC alterations without any detectable inflammatory infiltrate throughout the neuromuscular layer.

The main findings for each of these patterns are detailed in a previously published paper (24). A normal morphology was detected in jejunal samples from all control patients.

Interganglionic distance between myenteric ganglia. The distance between myenteric ganglia was calculated on adjacent microscopic fields in random sections. All consecutive fields were analyzed from

the first detectable ganglion present on one extremity of a given section (beginning from the left side) toward the opposite site. At least three random (i.e., nonconsecutive) jejunal cross sections from one specimen per patient and per control were examined. Images (final magnification ×1,000) were captured with a Nikon DXM1200 digital camera system (Nikon, Tokyo, Japan) on a LEICA DM LB (Leica, Mannheim, Germany) light transmission microscope, coupled with the Automatic Camera Tamer (ACT)-1 dedicated software (Nikon). The distance between consecutive ganglia was calculated using the software ImageJ v. 1.48. Because the actual margins of each ganglion in paraffin-embedded tissue sections cannot be firmly defined, we elected to consider clusters of NSE immunoreactive neuronal cell bodies that were at a distance of less than 100, 200, 300, or 400 μm as a single arbitrary ganglionic unit. Each interganglionic distance allowed us to identify significant differences in terms of neuronal counts between pathological vs. control specimens. To establish a reproducible criterion for neuronal counts, we chose the 300-μm distance, because, among the various ranges used in our paper, previous ancillary experiments led us to conclude that this was the closest interganglionic distance best fitting with the distance between ganglia evaluated by qualitative analysis (data not shown). The quantitative data were correlated with symptoms and signs of patients with severe dysmotility (Fig. 1).

Neuronal cell body count per myenteric and submucosal ganglion. Myenteric and submucosal NSE immunoreactive neuronal cell bodies were counted per ganglion at ×4,000 final magnification with a light transmission microscope (Olympus AX 70; Olympus, Melville, NY)

by three investigators (E. Bos, A. G., and R. De G., blinded in terms of any clinical features or histopathological group from which the examined sections derived). Focusing on the neuromuscular ridge and moving along the myenteric ganglia as well as throughout the submucosal layer for related ganglia, we evaluated consecutive microscopic fields (at least 20). Each blinded operator counted the total number of NSE immunoreactive neuronal cell bodies/ganglion. Figure 2 shows representative examples of the sections and magnification used for the neuronal count in the neuromuscular layer (Fig. 2A) and in the submucosa (Fig. 2B).

Interobserver variability for myenteric and submucosal neuronal cell body count. To assess the interobserver variability of this technique, the final number of neuronal cell bodies/ganglion per patient was calculated in myenteric and submucosal ganglia by each operator. For myenteric ganglia, concordance among the data was defined when the difference in the mean number from each single count was no more than five neurons, whereas a difference of more than five neurons was defined as discordant. Because of the limited number of neuronal cell bodies in submucosal ganglia, a mean number difference from each single count no more than one neuron was considered concordant. To test the power of the method among observers, the mean value of myenteric neurons per ganglion of samples that did not reach concordance ($n = 8$) was included in the study. Since the mean value of neurons calculated in patients with dysmotility was still very far from the mean value of neurons in controls, the samples that did not reach agreement were not outliers.
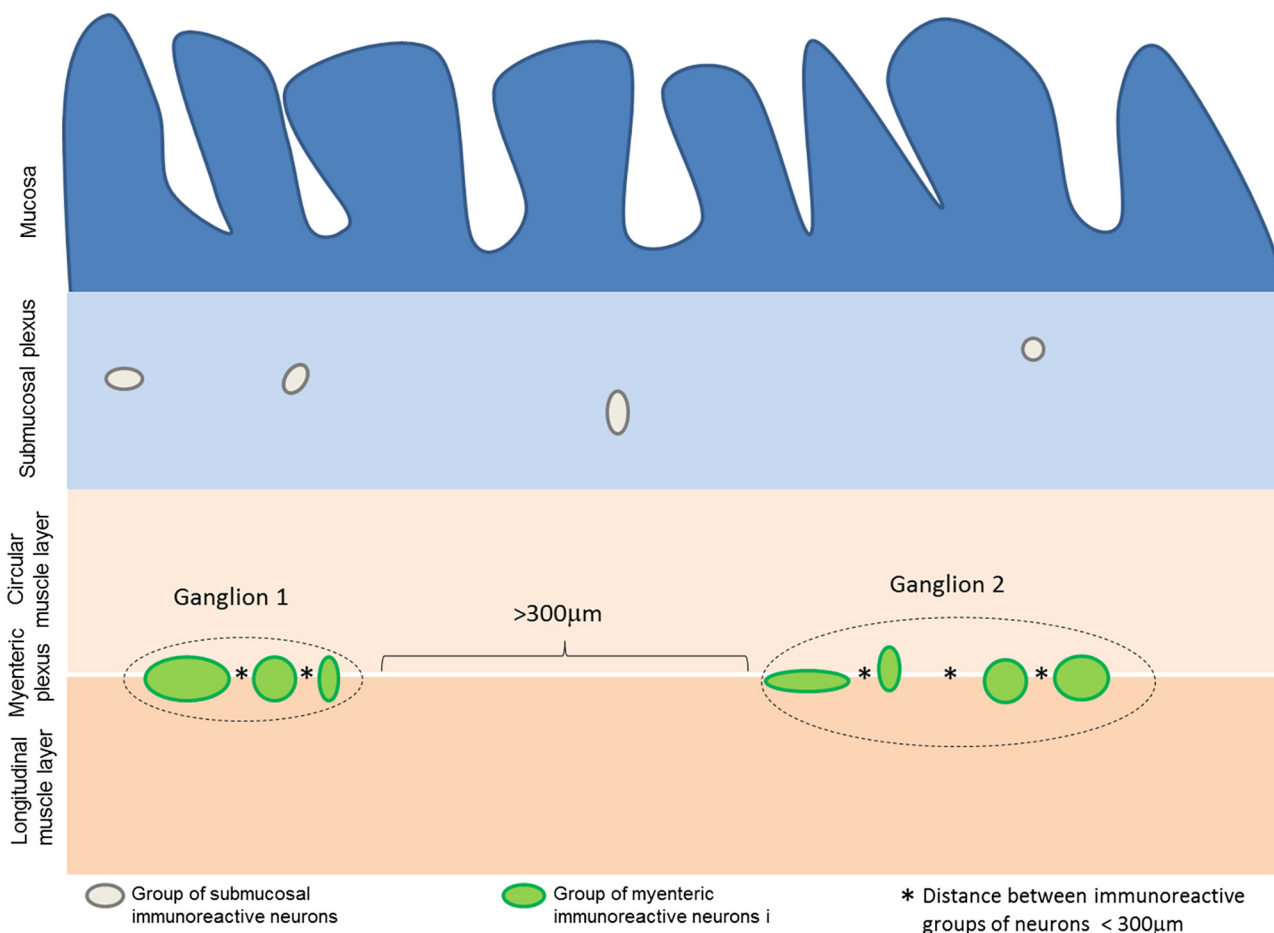
Fig. 1. Measurement of interganglionic distance. Schematic representation of the method by which interganglionic distances were defined, using the 300-μm cut-off value. Groups of immunoreactive neurons separated by less than 300 μm (distances indicated by *) were considered part of the same arbitrary ganglionic unit. Distances ≥300 μm were used as the threshold value to distinguish two different ganglia (indicated by square brackets).
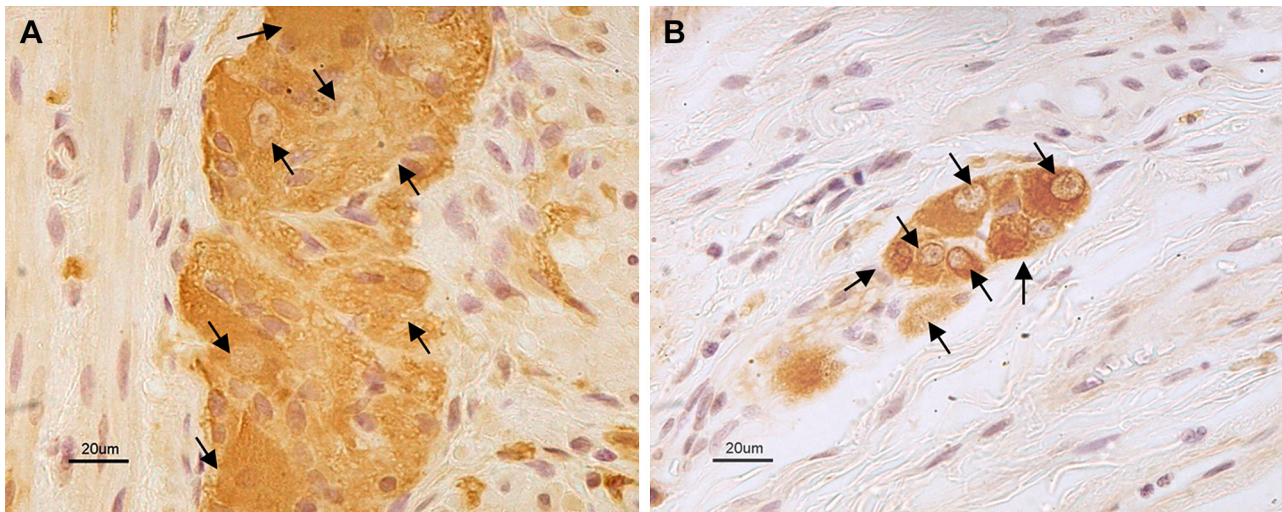
Fig. 2. Neurons identified by a pan-neuronal marker in myenteric and submucosal plexuses. Representative photomicrographs showing neuron-specific enolase (NSE) immunolabeling in the myenteric (*A*) and submucosal (*B*) plexus of a control sample. Black arrows indicate identified neuronal cell bodies.

Statistical analysis. The statistical analysis was performed using the free Software R-Cran (v. 3.5.2; Free Software Foundation's GNU project). To evaluate the differences between means (SD) of myenteric and submucosal neurons, as well as interganglionic distance, the following tests were applied: *1*) Mann-Whitney *U* test to compare severe dismotility vs. controls; *2*) Kruskal-Wallis coupled with a secondary Dunn's comparative test for multiple group comparisons was used to assess the three main groups, i.e., CIPO vs. enteric dysmotility vs. controls and AN vs. INF vs. DEG vs. controls). Univariate and multivariate nonparametric linear regression tests were carried out to identify possible correlations between morphometric and clinical data.

RESULTS

Interganglionic distance in myenteric ganglia. When we used 300 μm as the cut-off distance between two adjacent myenteric ganglia, sections of patients with severe dysmotility (as a whole) exhibited a significantly increased interganglionic distance compared with controls ($P = 0.0005$; Fig. 3, *A, D,* and *F*). The interganglionic distances in patients with enteric dysmotility or CIPO (Fig. 3*B*) were also significantly increased compared with controls ($P = 0.0076$ and $P = 0.0001$, respectively; Kruskal-Wallis $P = 0.0009$). There were no differences in interganglionic distance between patients with enteric dysmotility or CIPO. Similarly, the interganglionic distance in patients with with AN, INF, or DEG CIPO (Fig. 3*C*) was significantly increased compared with controls ($P = 0.0099$; $P = 0.0004$, and $P = 0.0008$, respectively; Kruskal-Wallis $P = 0.0035$). The comparison of interganglionic distances among AN, INF, and DEG histopathological subgroups did not show significant differences.

Myenteric and submucosal neuronal counts. Compared with controls, patients with severe dysmotility showed a 2.2-fold decrease in the number of neurons per ganglion in myenteric plexus ($P < 0.00001$) and a 1.6-fold decrease in submucosal plexus ($P < 0.0004$; Fig. 4, *A* and *B*). Similarly, in enteric dysmotility and CIPO subgroups, neurons decreased 2.2-fold vs. controls in myenteric plexus ($P < 0.00001$ and $P = 0.0001$; Kruskal-Wallis $P < 0.00001$) and 1.6-fold in submucosal plexus ($P = 0.0014$ and $P = 0.0002$, respectively; Kruskal-

Wallis $P = 0.0013$) with no difference between the two subgroups (Fig. 4, *C* and *D*). Quantitative analysis of enteric neurons in patients with severe dysmotility subdivided into the three histopathologically defined subsets (Fig. 4, *E* and *F*) showed that neurons in myenteric plexus decreased 1.9-fold in AN, 2.3-fold in INF, and 2.6-fold in DEG vs. controls ($P = 0.0106$, $P < 0.00001$, and $P < 0.00001$, respectively; Kruskal-Wallis $P < 0.00001$). Furthermore, INF and DEG showed fewer myenteric neurons than AN ($P = 0.0390$ and $P = 0.008$). The number of neurons/ganglion calculated in submucosal plexus were decreased 1.7-fold in AN, 1.6-fold in INF, and 1.4-fold in DEG vs. controls ($P = 0.0001$, $P = 0.0003$, $P = 0.0496$, respectively; Kruskal-Wallis $P = 0.0006$).

The final concordance of neuronal cell counts in myenteric plexus of severe dysmotility and controls, obtained comparing the final results of each operator, was 80% for the total 40 cases (patients and controls) analyzed in this study. The final concordance of neuronal count in submucosal plexus was 97.5%.

Correlation among symptoms, neuronal counts, and interganglionic distances. The number of subocclusive episodes increased in INF and DEG vs. controls ($P = 0.0025$ and $P = 0.0022$; Kruskal-Wallis $P < 0.01$) but not in AN subgroup (Fig. 5*A*).

Data analysis showed correlations between the number of both myenteric and submucosal neurons per ganglion and various morphometric and clinical parameters.

Univariate analysis indicated that the myenteric interganglionic distance was inversely correlated with the number of myenteric neurons ($t = -2.953$, $P = 0.006$); and directly correlated with the number of subocclusive episodes ($t = 4.54$, $P < 0.001$). Abdominal distension was inversely correlated with the number of neurons/ganglion in both myenteric and submucosal plexuses and directly correlated with the interganglionic distance ($t = -6.066$, $P < 0.0001$; $t = -3.768$, $P = 0.001$; $t = 2.268$, $P = 0.029$). Symptoms showing an inverse correlation with the number of neurons/ganglion in both myenteric and submucosal plexuses included pain ($t = -4.947$, $P < 0.0001$; $t = -03.692$, $P = 0.001$); early satiety ($t = -2.983$, $P = 0.005$; $t = -2.16$, $P = 0.038$), and constipation
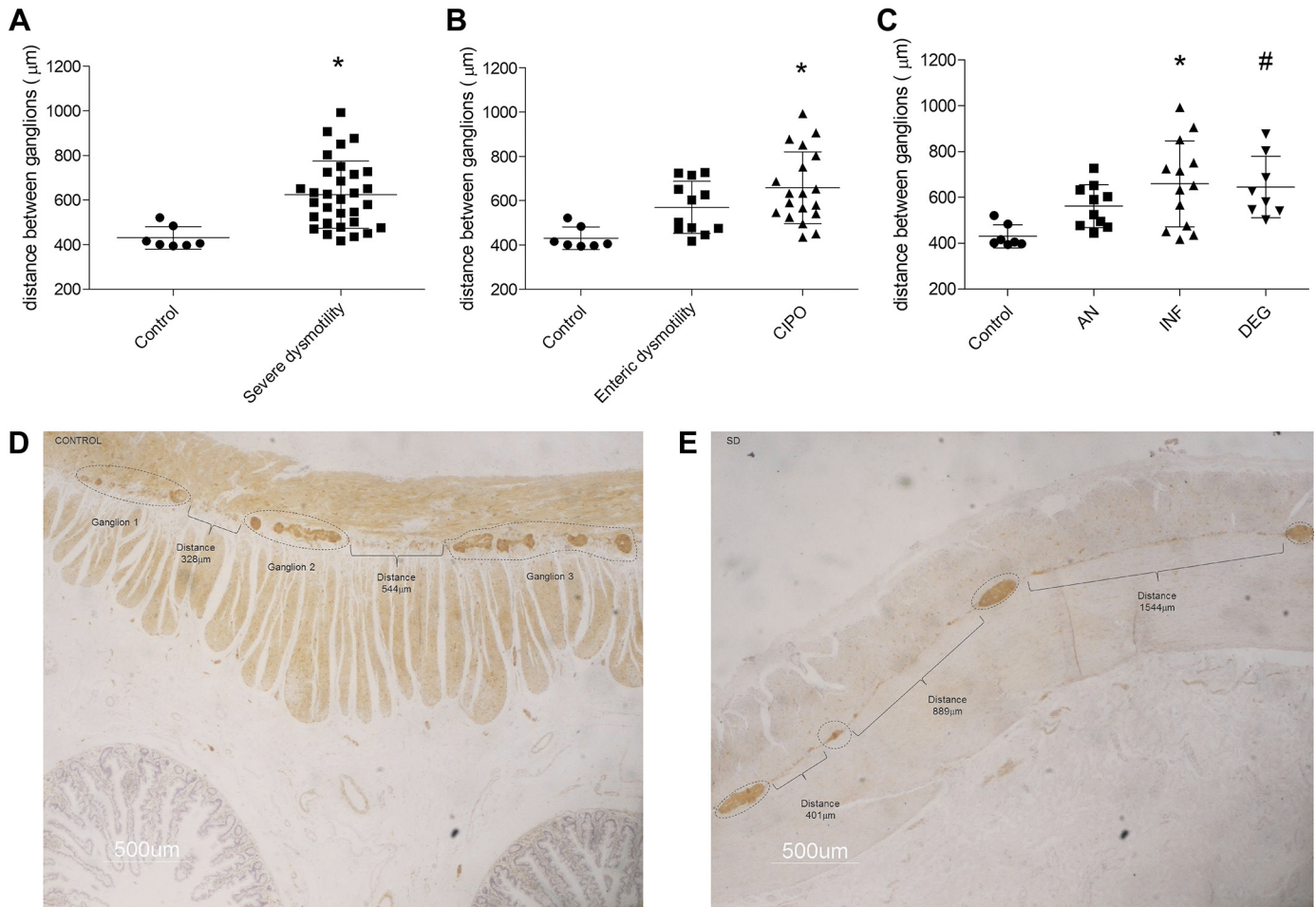
Fig. 3. Interganglionic distance in myenteric ganglia. Distance between ganglia using the 300-μm threshold comparing controls (622.3 ± 151.8 μm) and patients with severe dysmotility (427.4 ± 46.8 μm), *P = 0.0005 (A), enteric dysmotility (569.8 ± 117.7 μm) and CIPO (653.3 ± 164.7 μm), *P = 0.0076 and #P = 0.0001 (B), and apparently normal (AN; 562.1 ± 93.2 μm), inflammatory neuromyopathy (INF; 651.3 ± 190.6 μm), and degenerative neuromyopathy (DEG; 645.25 ± 134.2 μm), *P = 0.0099, #P = 0.0004, and §P = 0.0008 (C). *Bottom*: examples of interganglionic distance measurements using ImageJ software for a control sample (D) and a patient with severe dysmotility (E). Neuron-specific enolase (NSE) immunostaining; 500 μm final magnification.

($t = -3.215$, $P = 0.03$; $t = -2.907$, $P = 0.006$). Finally, SIBO and nausea correlated with the interganglionic distance ($t = 2.219$, $P = 0.033$; $t = 2.547$, $P = 0.015$).

Multivariate analysis of all covariates that had a significant value at univariate analysis, identified a correlation between the interganglionic distance and the number of intestinal sub-occlusive episodes ($t = 2.742$, $P < 0.01$; Fig. 5B) and an inverse correlation between the number of neurons/ganglion in myenteric plexus and abdominal distension ($t = -2.542$, $P = 0.0167$).

DISCUSSION

A complex integration among different regulatory cell types in the GI tract, including neurons and ICCs, is essential for the coordination of smooth muscle activity, thereby tuning GI motor function and propulsion (16, 30, 36). Various environmental noxae and genetic factors may disrupt the delicate equilibrium underlying the physiology of gut function and cause dysmotility (3, 11, 18). Enteric neurons exert a dominant role in the control of GI motility (16); thus, clinical conditions characterized by altered GI motility patterns are often referred to as enteric neuropathies (32). Enteric neuropathies can be

suspected by altered small bowel or colonic manometry or by qualitative histopathological alterations with or without morphometric analysis of the number of enteric neurons. Although whole mount preparations represent the gold standard for submucosal and myenteric neuron quantitative analysis (12, 14, 26, 34), more readily available, routinely collected, paraffin-embedded specimens may provide useful information on enteric neuron number. However, the validation of a standard method for quantitative analysis of enteric neurons on paraffin-embedded sections has long been debated among enteric neuropathologists to better characterize patients with neurogenic intestinal dysmotility (3). In this morphometric study, we aimed to establish a method that would allow us to use paraffin-embedded tissue samples for quantitative analysis taking into account the number of neuronal cell bodies/(myenteric and submucosal) ganglion as well as the distance between two adjacent myenteric ganglia in jejunal specimens of patients with severe forms of gut dysmotility compared with controls. To overcome the difficulty of establishing the margin of each individual ganglion in bidimensional tissue preparations such as paraffin sections, we tested distances (from 100 to 400 μm) between two clusters of myenteric neurons identified with a
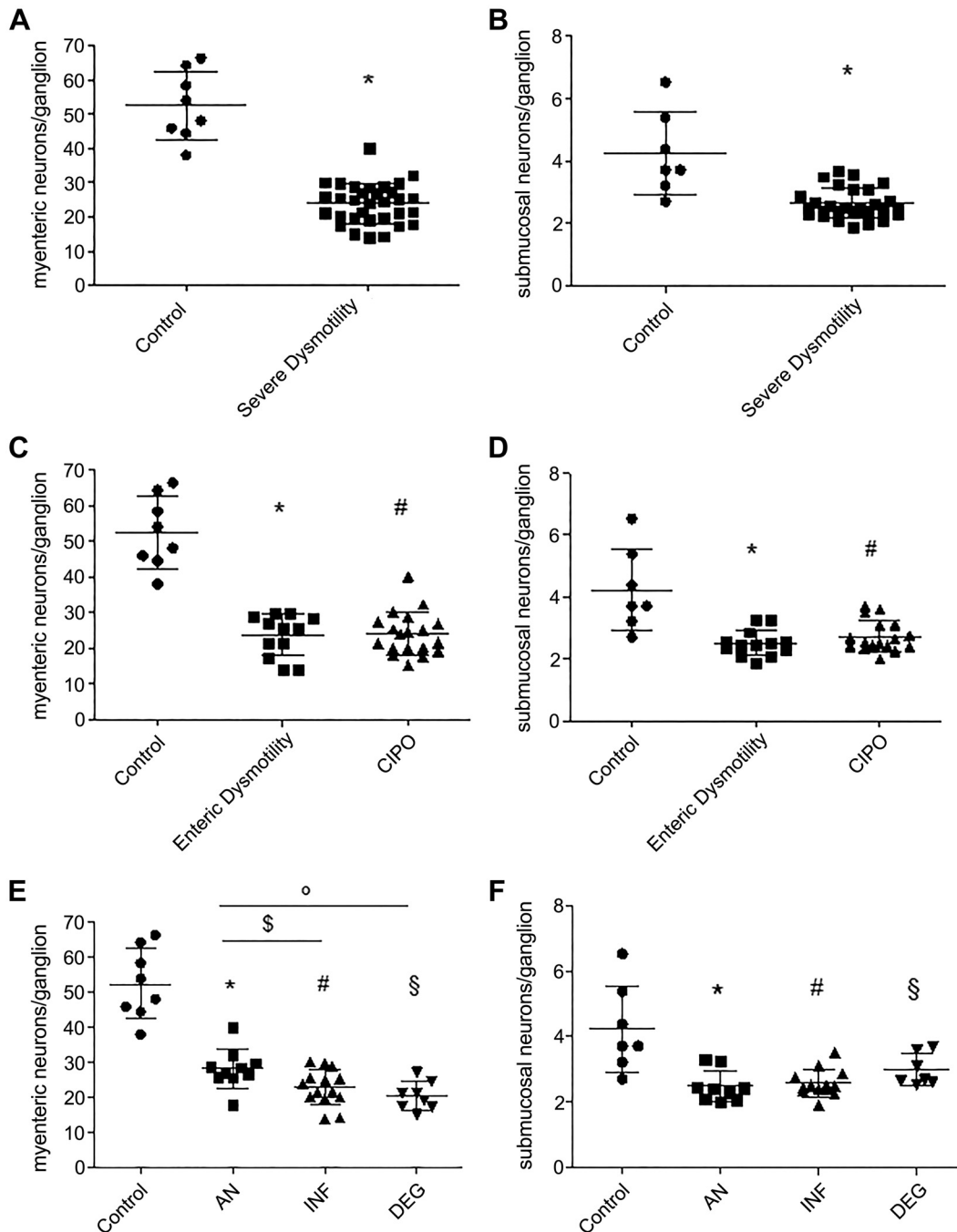
Fig. 4. Myenteric and submucosal neuronal cell counts in patients with severe dysmotility and controls. *A*: myenteric neurons counted in the whole severe dysmotility (24.0 ± 5.8 neurons/ganglion) group vs. controls (52.4 ± 10.0 neurons/ganglions), *P < 0.00001. *B*: submucosal neurons counted in the whole severe dysmotility (2.6 ± 0.5 neurons/ganglion) group vs. controls (4.2 ± 1.3 neurons/ganglion), *P = 0.0004. *C*: myenteric neuronal counts in enteric dysmotility (ED; 23.8 ± 5.5 neurons/ganglion) and chronic intestinal pseudo-obstruction (CIPO; 24.0 ± 6.0 neurons/ganglion) subgroups, *P < 0.00001 and #P < 0.0001. *D*: submucosal neuronal counts in ED (2.5 ± 0.4 neurons/ganglion) and CIPO (2.7 ± 0.5 neurons/ganglion) subgroups,*P = 0.0014 and #P = 0.0002. *E*: myenteric neuronal counts in apparently normal (AN; 28.3 ± 5.6 neurons/ganglion), inflammatory neuromyopathy (INF; 22.9 ± 5.6 neurons/ganglion), and degenerative neuromyopathy (DEG; 20.4 ± 4.0 neurons/ganglion) subgroups, *P = 0.0106, #§P < 0.00001, $$P$ = 0.0390, and °P = 0.008. *F*: submucosal neuronal counts in AN (2.5 ± 0.5 neurons/ganglion), INF (2.6 ± 0.4 neurons/ganglion), and DEG (3.0 ± 10.5 neurons/ganglion) subgroups, *P < 0.0001, #P = 0.0003, and §P = 0.0496.

pan-neuronal marker within a ganglion to distinguish patients' (disease) vs. controls' (normal) specimens and elected to use a 300-μm interganglionic distance to quantify the number of myenteric neurons/ganglion. Notably, this quantitative method showed a very low variability among different operators, and,

if further validated in a large cohort of samples, it will hopefully provide a reliable diagnostic tool for patients with severe neurogenic dysmotility.

Except from guidelines by an international working group on gut tissue collection, handling, and histopathological report-

Fig. 5. Number of subocclusive episodes distribution among immunohistochemically defined subgroups and relationship with interganglionic distance. *A*: number of subocclusive episodes recorded per patient before surgical intervention. Patients were clustered accordingly with the qualitative immunohistochemically defined assessment. *P = 0.0025 and #P = 0.0022. *B*: scatter plot illustrating the relationship between number of subocclusive episodes and interganglionic distances.

ing of patients with gut dysmotility (18), there are no indications as to how a neuronal quantitative analysis should be performed on formalin-fixed, paraffin embedded specimens, the most commonly available material in any pathology unit. The lack of a standardized quantitative method is the main reason behind the wide variability reported so far in studies where neuronal counting has been attempted using tissue specimens of patients with gut motility disorders (3). Boyer et al. (5) compared neuronal assessment in whole mounts vs. paraffin-embedded tissue sections in a mouse model of dinitrobenzene sulfonic acid-induced colitis. The results, expressed as neuronal cell body/ganglion in paraffin-processed material, and as neurons per square millimeter in whole mounts, showed, as expected, marked differences in absolute numbers due to the different methods, but the percentage of neuronal cell loss was quite similar to that of the two quantitative approaches, thus demonstrating the validity of both methods for the determination of neuropathological changes.

One of the main issues in neuronal cell body number evaluation in paraffin material is about data normalization. Many methods have been attempted, but a standard consensus has not been achieved. Ippolito et al. (17) quantified myenteric neurons in paraffin section of human left colon in a control population, reporting the number of neurons as Σ neurons identified by the pan-neuronal marker HuC/D/Σ ganglionic area. Since myenteric ganglia are variable in size/area depending on the number of contained neurons or glial cells (13, 29, 37), this quantitative method may yield misleading results when one is comparing tissues from dysmotility patients to controls. Mandic et al. (25) measured the number of myenteric neurons per square centimeter of surface of the esophagus, stomach, duodenum, jejunum, ileum, transverse colon, and rectum in paraffin control tissue samples. However, a potential limitation of this method, which measures neurons normalized per microscopic field, is neuronal overestimation because of the inclusion of extraganglionic myenteric perikarya, which have been demonstrated to increase progressively with age (1). Based on these data, enteric neuron counts fit best when normalized per ganglion, although this does not overcome the problem of differences in ganglion size. However, this approach implies a definition of ganglion (1, 29) that is difficult

due to the lobulated silhouette of the human myenteric ganglia that often prevents an accurate definition of the ganglionic perimeter. Pathologists have suggested to define the border of a ganglion when one or more neurons and glial cells are surrounded by perineural cells (15). A shortfall of this criterion, however, is the finding that neurons can also be found in tertiary nerve fiber strands in the human colon (34). Other definitions of a myenteric ganglion include the detection of two or more adjacent ganglion cell bodies (2) or the presence of a minimum of three neuronal cell bodies with an interperikarya distance not exceeding two cell body diameters (6). Our approach to overcome the difficulty of defining ganglion actual margins using paraffin-embedded material and microtome sections was to define arbitrary myenteric ganglionic units as clusters of neurons separated by a fixed distance that allowed us to identify significant differences in neuronal counts between pathological and control specimens.

A key accuracy factor when estimating the number of myenteric and submucosal neurons is the reproducibility in terms of interobserver-variability. In this study, the concordance among the three investigators was defined as a cut-off of up to five myenteric neuron cell bodies, i.e., about five times lower than the difference between controls and severe dysmotility patients. The interobserver concordance was reached when the final measurement of each operator did not exceed five neuronal cell bodies from the average of three assessments. Using this cut off we had only 20% discordance. Furthermore, among the group of discordant samples (8/40), seven cases had six to ten neuronal cell bodies above the concordant limit of five, whereas only one was discordant for more than ten neuronal cell bodies. However, the estimated discordance (20%) did not affect the final quantitative results because of the stringent cut-off number (i.e., ≤5) of myenteric neurons used to establish interobserver agreement.

In our study, we detected a marked loss of myenteric neurons in all patients with severe dysmotility, which was similar for the two clinically relevant phenotypes, CIPO and enteric dysmotility, and for the three histopathological subtypes, i.e., AN, INF, and DEG. Our data, showing a substantive reduction (~50%) of both myenteric and submucosal neurons, are in agreement with the few previously reported quantitative

data in tissues of patients with severe dysmotility, including (28, 31) infants/children with CIPO (21). Although the submucosal plexus does not play a central role in controlling gastrointestinal motility, the neuronal loss also affected the submucosal plexus. The decrease of neuronal cell bodies involved both type of ganglia in the jejunum of patients with severe dysmotility.

Another significant morphometric result in our study is that the decreased number of myenteric neurons correlated with the increase of interganglionic distance. Compared with controls, the distance between adjacent myenteric ganglia was increased by ~40% in severe dysmotility (either enteric dysmotility or CIPO) and in histochemically distinct severe dysmotility subsets. From a clinical point of view, the distance between ganglia may have considerable diagnostic potential since ~76% of patients with severe dysmotility can be identified by interganglionic distance and the remaining 24% by adding the quantitative analysis of neuronal number per ganglion. Future studies based on a large control sample size, taking into account sex- and age-related factors, are needed to establish the interganglionic distance range of control (normal manometric pattern/absence of symptoms) subjects and validate objective criteria for the diagnosis of enteric neuropathies. We believe that an ideal quantitative approach should include the interganglionic distance as a first parameter, followed by neuronal cell count in patients with normal interganglionic distance. Furthermore, in our study, the increased interganglionic distance correlated with a higher number of intestinal subocclusive episodes, thus implying that the distance between myenteric ganglia might indicate the most severe forms of dysmotility. In addition, the altered GI motility and the worsening of gut dysmotility, as reflected by an increased abdominal distension (7), were associated with at least 50% neuronal loss in the small intestine. Overall, our data indicate that the clinical manifestations and their severity increase as the myenteric neuronal number decreases and the interganglionic distance increases. The 50% loss of neuronal cell bodies in myenteric and submucosal ganglia suggests a critical mass of neurons necessary to maintain intestinal motility within normal range, though this needs to be confirmed in large sample size of patients. Finally, the histochemically defined AN subset showed a significant increase in interganglionic distance along with the loss of myenteric and submucosal neurons per ganglion, the latter being less pronounced in comparison with INF and DEG. AN was also associated with a lower number of intestinal subocclusive episodes (vs. the other two CIPO subsets). Taken together, the quantitative findings may explain the clinical manifestations and the abnormal manometric patterns detected in the AN group as previously published (24). The significant difference in neuronal cell body counts per ganglion between AN and DEG or between AN and INF suggests that the AN group may represent the initial stage of degenerative or inflammatory processes, possibly evolving to the corresponding neuropathy identifiable with standard histopathological staining methods.

In conclusion, our study provides new, relatively simple neuronal morphometric approaches for paraffin sections obtained from patients with severe dysmotility and abnormal intestinal manometry. Compared with controls, the definition of increased interganglionic distance may be a criterion to help diagnosis and to reserve the more cumbersome quantitative analysis of neuronal cell bodies per ganglion to patients with an interganglionic distance within the range of controls. Patients who are labeled "apparently normal" by qualitative immunohistochemistry may have underlying quantitative interganglionic and neuronal number changes bearing clinically meaningful information.

DISCLAIMERS

The funding bodies did not influence the content of this article.

DISCLOSURES

R. De Georgio has participated as a consultant for Shire, Sucampo, Coloplast, Kyowa Kirin International, and Takeda and received grant support from Shire and Takeda. These consultancies did not influence the content of this article. The other authors declare no conflict of interest.

AUTHOR CONTRIBUTIONS

E. Boschetti, V.S., C.S., and R.D.G. conceived and designed research; E. Boschetti, C.M., R.F.C., A.G., F.G., F.B., V.T., and P.C. performed experiments; E. Boschetti, C.M., A.A., J.R.M., R.F.C., A.G., E. Bonora, F.G., F.B., V.T., P.C., F.A., C.S., and R.D.G. analyzed data; E. Boschetti, C.M., A.A., J.R.M., R.F.C., E. Bonora, F.A., V.S., C.S., and R.D.G. interpreted results of experiments; E. Boschetti prepared figures; E. Boschetti, A.A., J.R.M., F.G., F.A., C.S., and R.D.G. drafted manuscript; E. Boschetti, C.M., A.A., J.R.M., R.F.C., E. Bonora, F.A., V.S., C.S., and R.D.G. edited and revised manuscript; E. Boschetti, C.M., A.A., J.R.M., R.F.C., A.G., E. Bonora, F.G., F.B., V.T., P.C., F.A., V.S., C.S., and R.D.G. approved final version of manuscript.

REFERENCES

1. **Abalo R, José Rivera A, Vera G, Isabel Martín M.** Ileal myenteric plexus in aged guinea-pigs: loss of structure and calretinin-immunoreactive neurones. *Neurogastroenterol Motil* 17: 123–132, 2005. doi:10.1111/j.1365-2982.2004.00612.x.
2. **Bernard CE, Gibbons SJ, Gomez-Pinilla PJ, Lurken MS, Schmalz PF, Roeder JL, Linden D, Cima RR, Dozois EJ, Larson DW, Camilleri M, Zinsmeister AR, Pozo MJ, Hicks GA, Farrugia G.** Effect of age on the enteric nervous system of the human colon. *Neurogastroenterol Motil* 21: 746–e46, 2009. doi:10.1111/j.1365-2982.2008.01245.x.
3. **Bernardini N, Ippolito C, Segnani C, Mattii L, Bassotti G, Villanacci V, Blandizzi C, Dolfi A.** Histopathology in gastrointestinal neuromuscular diseases: methodological and ontological issues. *Adv Anat Pathol* 20: 17–31, 2013. doi:10.1097/PAP.0b013e31827b65c0.
4. **Bernardini N, Segnani C, Ippolito C, De Giorgio R, Colucci R, Faussone-Pellegrini MS, Chiarugi M, Campani D, Castagna M, Mattii L, Blandizzi C, Dolfi A.** Immunohistochemical analysis of myenteric ganglia and interstitial cells of Cajal in ulcerative colitis. *J Cell Mol Med* 16: 318–327, 2012. doi:10.1111/j.1582-4934.2011.01298.x.
5. **Boyer L, Ghoreishi M, Templeman V, Vallance BA, Buchan AM, Jevon G, Jacobson K.** Myenteric plexus injury and apoptosis in experimental colitis. *Auton Neurosci* 117: 41–53, 2005. doi:10.1016/j.autneu.2004.10.006.
6. **Coerdt W, Michel JS, Rippin G, Kletzki S, Gerein V, Müntefering H, Arnemann J.** Quantitative morphometric analysis of the submucous plexus in age-related control groups. *Virchows Arch* 444: 239–246, 2004. doi:10.1007/s00428-003-0951-7.
7. **Cogliandro RF, Antonucci A, De Giorgio R, Barbara G, Cremon C, Cogliandro L, Frisoni C, Pezzilli R, Morselli-Labate AM, Corinaldesi**

R, Stanghellini V. Patient-reported outcomes and gut dysmotility in functional gastrointestinal disorders. *Neurogastroenterol Motil* 23: 1084–1091, 2011. doi:10.1111/j.1365-2982.2011.01783.x.

8. **De Giorgio R, Sarnelli G, Corinaldesi R, Stanghellini V.** Advances in our understanding of the pathology of chronic intestinal pseudo-obstruction. *Gut* 53: 1549–1552, 2004. doi:10.1136/gut.2004.043968.

9. **Di Nardo G, Di Lorenzo C, Lauro A, Stanghellini V, Thapar N, Karunaratne TB, Volta U, De Giorgio R.** Chronic intestinal pseudo-obstruction in children and adults: diagnosis and therapeutic options. *Neurogastroenterol Motil* 29: e12945, 2017. doi:10.1111/nmo.12945.

10. **Doleshal M, Magotra AA, Choudhury B, Cannon BD, Labourier E, Szafranska AE.** Evaluation and validation of total RNA extraction methods for microRNA expression analyses in formalin-fixed, paraffin-embedded tissues. *J Mol Diagn* 10: 203–211, 2008. doi:10.2353/jmoldx.2008.070153.

11. **Downes TJ, Cheruvu MS, Karunaratne TB, De Giorgio R, Farmer AD.** Pathophysiology, Diagnosis, and Management of Chronic Intestinal Pseudo-Obstruction. *J Clin Gastroenterol* 52: 477–489, 2018. doi:10.1097/MCG.0000000000001047.

12. **Gabella G.** The number of neurons in the small intestine of mice, guinea-pigs and sheep. *Neuroscience* 22: 737–752, 1987. doi:10.1016/0306-4522(87)90369-1.

13. **Gabella G, Trigg P.** Size of neurons and glial cells in the enteric ganglia of mice, guinea-pigs, rabbits and sheep. *J Neurocytol* 13: 49–71, 1984. doi:10.1007/BF01148318.

14. **Ganns D, Schrödl F, Neuhuber W, Brehmer A.** Investigation of general and cytoskeletal markers to estimate numbers and proportions of neurons in the human intestine. *Histol Histopathol* 21: 41–51, 2006. doi:10.14670/HH-21.41.

15. **Hoyle CH, Burnstock G.** Neuronal populations in the submucous plexus of the human colon. *J Anat* 166: 7–22, 1989.

16. **Hu H, Spencer NJ.** Enteric nervous system structure and neurochemistry related to function and neuropathology. In: *Physiology of the Gastrointestinal Tract* (6th ed.), edited by Said HM. Atlanta, GA: Elsevier, 2018. doi:10.1016/C2015-1-04889-X.

17. **Ippolito C, Segnani C, De Giorgio R, Blandizzi C, Mattii L, Castagna M, Moscato S, Dolfi A, Bernardini N.** Quantitative evaluation of myenteric ganglion cells in normal human left colon: implications for histopathological analysis. *Cell Tissue Res* 336: 191–201, 2009. doi:10.1007/s00441-009-0770-5.

18. **Knowles CH, De Giorgio R, Kapur RP, Bruder E, Farrugia G, Geboes K, Gershon MD, Hutson J, Lindberg G, Martin JE, Meier-Ruge WA, Milla PJ, Smith VV, Vandervinden JM, Veress B, Wedel T.** Gastrointestinal neuromuscular pathology: guidelines for histological techniques and reporting on behalf of the Gastro 2009 International Working Group. *Acta Neuropathol* 118: 271–301, 2009. doi:10.1007/s00401-009-0527-y.

19. **Knowles CH, De Giorgio R, Kapur RP, Bruder E, Farrugia G, Geboes K, Lindberg G, Martin JE, Meier-Ruge WA, Milla PJ, Smith VV, Vandervinden JM, Veress B, Wedel T.** The London Classification of gastrointestinal neuromuscular pathology: report on behalf of the Gastro 2009 International Working Group. *Gut* 59: 882–887, 2010. doi:10.1136/gut.2009.200444.

20. **Knowles CH, Veress B, Kapur RP, Wedel T, Farrugia G, Vanderwinden JM, Geboes K, Smith VV, Martin JE, Lindberg G, Milla PJ, De Giorgio R.** Quantitation of cellular components of the enteric nervous system in the normal human gastrointestinal tract--report on behalf of the Gastro 2009 International Working Group. *Neurogastroenterol Motil* 23: 115–124, 2011. doi:10.1111/j.1365-2982.2010.01657.x.

21. **Krishnamurthy S, Heng Y, Schuffler MD.** Chronic intestinal pseudo-obstruction in infants and children caused by diverse abnormalities of the myenteric plexus. *Gastroenterology* 104: 1398–1408, 1993. doi:10.1016/0016-5085(93)90348-G.

22. **Lindberg G, Iwarzon M, Tornblom H.** Clinical features and long-term survival in chronic intestinal pseudo-obstruction and enteric dysmotility. *Scand J Gastroenterol* 44: 692–699, 2009. doi:10.1080/00365520902839642.

23. **Lindberg G, Törnblom H, Iwarzon M, Nyberg B, Martin JE, Veress B.** Full-thickness biopsy findings in chronic intestinal pseudo-obstruction and enteric dysmotility. *Gut* 58: 1084–1090, 2009. doi:10.1136/gut.2008.148296.

24. **Malagelada C, Karunaratne TB, Accarino A, Cogliandro RF, Landolfi S, Gori A, Boschetti E, Malagelada JR, Stanghellini V, Azpiroz F, De Giorgio R.** Comparison between small bowel manometric patterns and full-thickness biopsy histopathology in severe intestinal dysmotility. *Neurogastroenterol Motil* 30: e13219, 2018. doi:10.1111/nmo.13219.

25. **Mandić P, Filipović T, Gasić M, Djukić-Macut N, Filipović M, Bogosavljević I.** Quantitative morphometric analysis of the myenteric nervous plexus ganglion structures along the human digestive tract. *Vojnosanit Pregl* 73: 559–565, 2016. doi:10.2298/VSP141231046M.

26. **Murphy EM, Defontgalland D, Costa M, Brookes SJ, Wattchow DA.** Quantification of subclasses of human colonic myenteric neurons by immunoreactivity to Hu, choline acetyltransferase and nitric oxide synthase. *Neurogastroenterol Motil* 19: 126–134, 2007. doi:10.1111/j.1365-2982.2006.00843.x.

27. **Murphy F, Paran TS, Puri P.** Orchidopexy and its impact on fertility. *Pediatr Surg Int* 23: 625–632, 2007. doi:10.1007/s00383-007-1900-3.

28. **Nagata T, Aoki M, Hasegawa T, Shiga Y, Hayashi T, Higuchi J, Abe K, Tanno T, Konno H, Itoyama Y.** [An autopsy case of atypical Friedreich's ataxia with chronic idiopathic intestinal pseudo-obstruction]. *Rinsho Shinkeigaku* 41: 412–417, 2001.

29. **Parr EJ, Sharkey KA.** The use of constitutive nuclear oncoproteins to count neurons in the enteric nervous system of the guinea pig. *Cell Tissue Res* 277: 325–331, 1994. doi:10.1007/BF00327780.

30. **Quigley EM.** What we have learned about colonic motility: normal and disturbed. *Curr Opin Gastroenterol* 26: 53–60, 2010. doi:10.1097/MOG.0b013e328332c977.

31. **Schuffler MD, Bird TD, Sumi SM, Cook A.** A familial neuronal disease presenting as intestinal pseudoobstruction. *Gastroenterology* 75: 889–898, 1978. doi:10.1016/0016-5085(78)90476-6.

32. **Spencer NJ, Dinning PG, Brookes SJ, Costa M.** Insights into the mechanisms underlying colonic motor patterns. *J Physiol* 594: 4099–4116, 2016. doi:10.1113/JP271919.

33. **Stanghellini V, Cogliandro RF, de Giorgio R, Barbara G, Salvioli B, Corinaldesi R.** Chronic intestinal pseudo-obstruction: manifestations, natural history and management. *Neurogastroenterol Motil* 19: 440–452, 2007. doi:10.1111/j.1365-2982.2007.00902.x.

34. **Wedel T, Roblick U, Gleiss J, Schiedeck T, Bruch HP, Kühnel W, Krammer HJ.** Organization of the enteric nervous system in the human colon demonstrated by wholemount immunohistochemistry with special reference to the submucous plexus. *Ann Anat* 181: 327–337, 1999. doi:10.1016/S0940-9602(99)80122-8.

35. **Wingate D, Hongo M, Kellow J, Lindberg G, Smout A.** Disorders of gastrointestinal motility: towards a new classification. *J Gastroenterol Hepatol* 17, *Suppl*: S1–S14, 2002. doi:10.1046/j.1440-1746.17.s1.7.x.

36. **Wood JD.** Enteric nervous system: reflexes, pattern generators and motility. *Curr Opin Gastroenterol* 24: 149–158, 2008. doi:10.1097/MOG.0b013e3282f56125.

37. **Young HM, Furness JB, Sewell P, Burcher EF, Kandiah CJ.** Total numbers of neurons in myenteric ganglia of the guinea-pig small intestine. *Cell Tissue Res* 272: 197–200, 1993. doi:10.1007/BF00323587.